Chemical Papers (2023) 77:3025–3034
https://doi.org/10.1007/s11696-023-02685-8

ORIGINAL PAPER

Development and photo-properties and intracellular behavior of visible-light-responsive molecule localizing to organelles of living cell

Kosei Shioji[1] · Masashi Ozaki[1] · Kasumi Kasai[1] · Hidefumi Iwashita[1] · Noriyoshi Nagahora[1] · Kentaro Okuma[1]

Received: 19 September 2022 / Accepted: 18 January 2023 / Published online: 2 February 2023

Abstract

Visible-light-responsive azobenzene derivative in which a functional group having cell membrane permeability and a fluorophore were bonded was synthesized. This compound localized to the hydrophobic part in the lipid membrane of the liposome, and when the light corresponding to the transition absorption of azobenzene was irradiated, morphological change of the liposome was observed. When this compound was loaded into living cells, this molecule localized to the lysosome and when irradiated with light of the same wavelength caused cell death. These observed changes are thought to be due to photoisomerization of azobenzene derivatives.

Graphical abstract

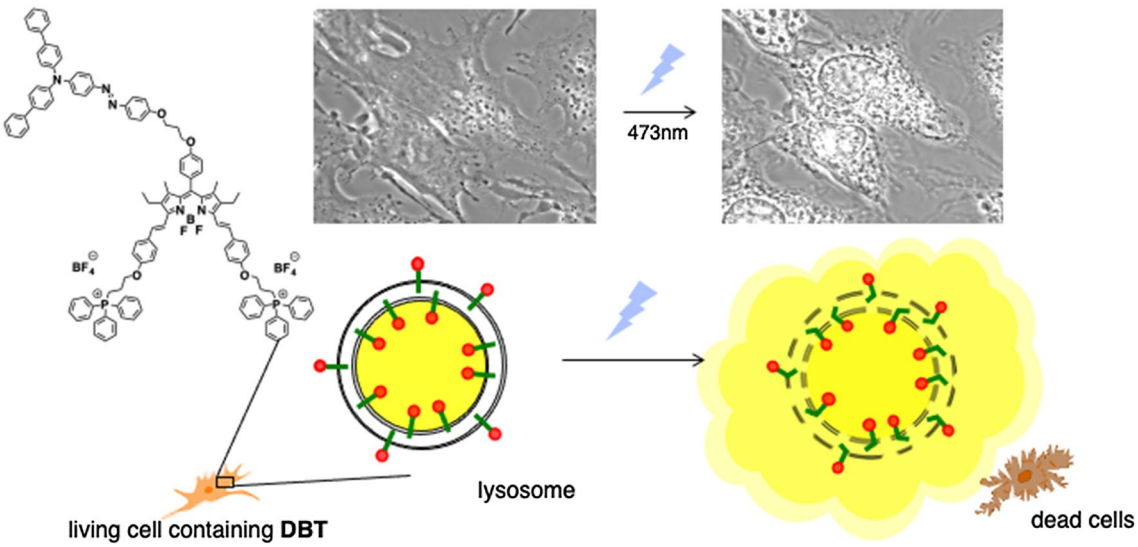

Keywords Azobenzene · Photo-isomerization · Liposome · Morhological change · Cell death

Abbreviations

AB	Azobenzene
BODIPY	Boron–dipyrromethene
DBAB	4-[Di(biphenyl-4-yl)amino] azobenzene
DBB	Dibenzoylbenzene
DIPEA	*N*,*N*-Diisopropylethylamine
DMSO	Dimethyl sulfoxide
DOPC	1,2-Dioleoyl-sn-glycero-3-phosphocholine
DPBF	Diphenylbenzofuran
EYPC	Egg-yolk phosphatidylcholine
GUV	Giant unilamellar vesicles

✉ Kosei Shioji
shioji@fukuoka-u.ac.jp

[1] Department of Chemistry, Faculty of Science, Fukuoka University, Jonan-Ku, Fukuoka 814-0180, Japan

HBSS	Hanks' balanced salt solution
HepG2	Human hepatocellular carcinoma
PTSA	P-toluenesulfonic acid
TPP	Triphenylphosphonium

Introduction

There are several organelles such as nucleus, mitochondria, lysosome and Golgi body in eukaryotic cells, and these organelles are separated by lipid membrane which was organized by weak interaction. The separation of organelles maintains the homeostasis of living cells. In order to understand the biological system, it is necessary to disturb the homeostasis (Stockwell 2004). Molecular genetics causes disturbance by regulating the expression level of a specific protein by genetic manipulation (Brenner 1974; Hartwell et al. 1991). On the other hand, an approach called chemical genetics has revealed the molecular mechanisms underlying biological processes by using organic small molecules instead of mutations and causing disturbance of biological systems (Schreiber 2003; Stockwell 2000). Disturbance using small organic molecules including peptides has been reported as inhibition of protein function (Kuruvilla et al. 2002), depolarization of mitochondria (Green et al. 2004), inhibition of translation in the process of protein synthesis (Tokala et al. 2018; Samundeeswari et al. 2017; Tacar et al. 2012) and disruption of the order of biological membranes (Felício et al. 2017). The findings obtained by these studies complement genetic understanding of biological systems and at the same time lead to understanding of epigenetic phenomena of living organisms.

Azobenzene and the related compounds undergo photoisomerization result in conformational change (Hartley 1937; Bandara et al. 2012; Merino et al. 2012; Banghart et al. 2004; Shinkai et al. 1983; Muraoka et al. 2003; Yu et al. 2003; Suzuki et al. 2012; Samanta et al. 2013; Lin et al. 2012; Wang et al. 2011; Beharry et al. 2011; Sebai et al. 2010; Sun et al. 2013; Hamada et al. 2005; Lee et al. 2012). It is reported that the isomerization of azobenzene derivatives causes dynamic disorder of phospholipid membrane, budding and bursting of lipid vesicles (Ishii et al. 2009; Diguet et al. 2012; Pernpeintner et al. 2017; Liu et al. 2017). These reports inspired to perform photo-manipulation of organic molecules in living cells. Azobenzene is isomerized from trans- to *cis*-form by absorbing ultraviolet radiation corresponding to π–π^* transition. The light irradiation at this wavelength itself causes damage to living cells. Nakano et al. have reported to azobenzene-based photochromic compounds responded to visible light. The use of this compound enables photoisomerization in living cells without photo-damage (Ando et al. 2003; Tanino et al. 2007; Nakano et al. 2012). For dynamic observation of azobenzene derivatives in living cells due to photoisomerization, it is necessary to synthesize molecules in which azobenzene derivatives are bounded with fluorophores which do not interfere with azobenzene transition. Previously, we reported morphological changes of vesicles using visible-light-responsive azobenzene derivatives (Kasai et al. 2022) In this study, a compound in which a fluorophore (BODIPY) (Loudet et al. 2007; Ulrich et al. 2008; Boens et al. 2012; Zhang et al. 2013) and a cell membrane permeability enhancing site (TPP) (Zhang et al. 2015) are bonded to DBAB which is a compound responsive to visible light was synthesized, and its optical properties, behaviors in cells and the effect of photoisomerization of the compounds on cells were observed (Fig. 1).

Materials and methods

Synthesis of DBT

Desired compound **DBT** was synthesized as follows: Using 4-nitroaniline and phenol as starting materials, azobenzene

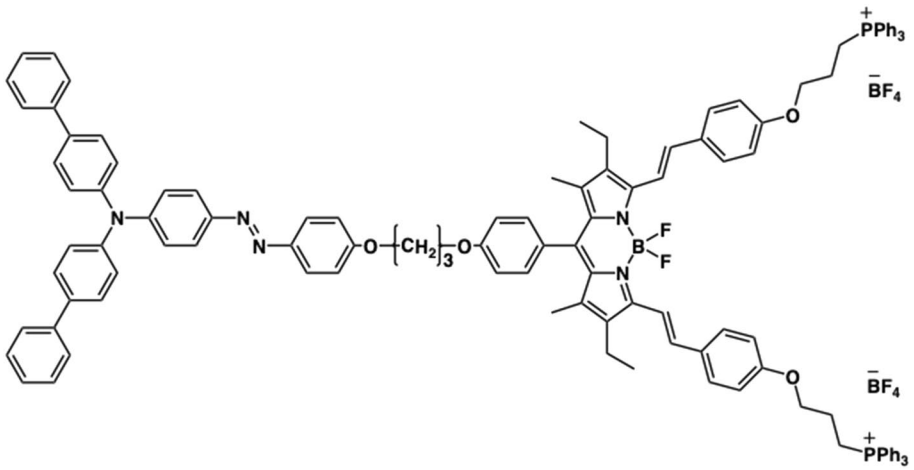

Fig. 1 Molecular design of **DBT**

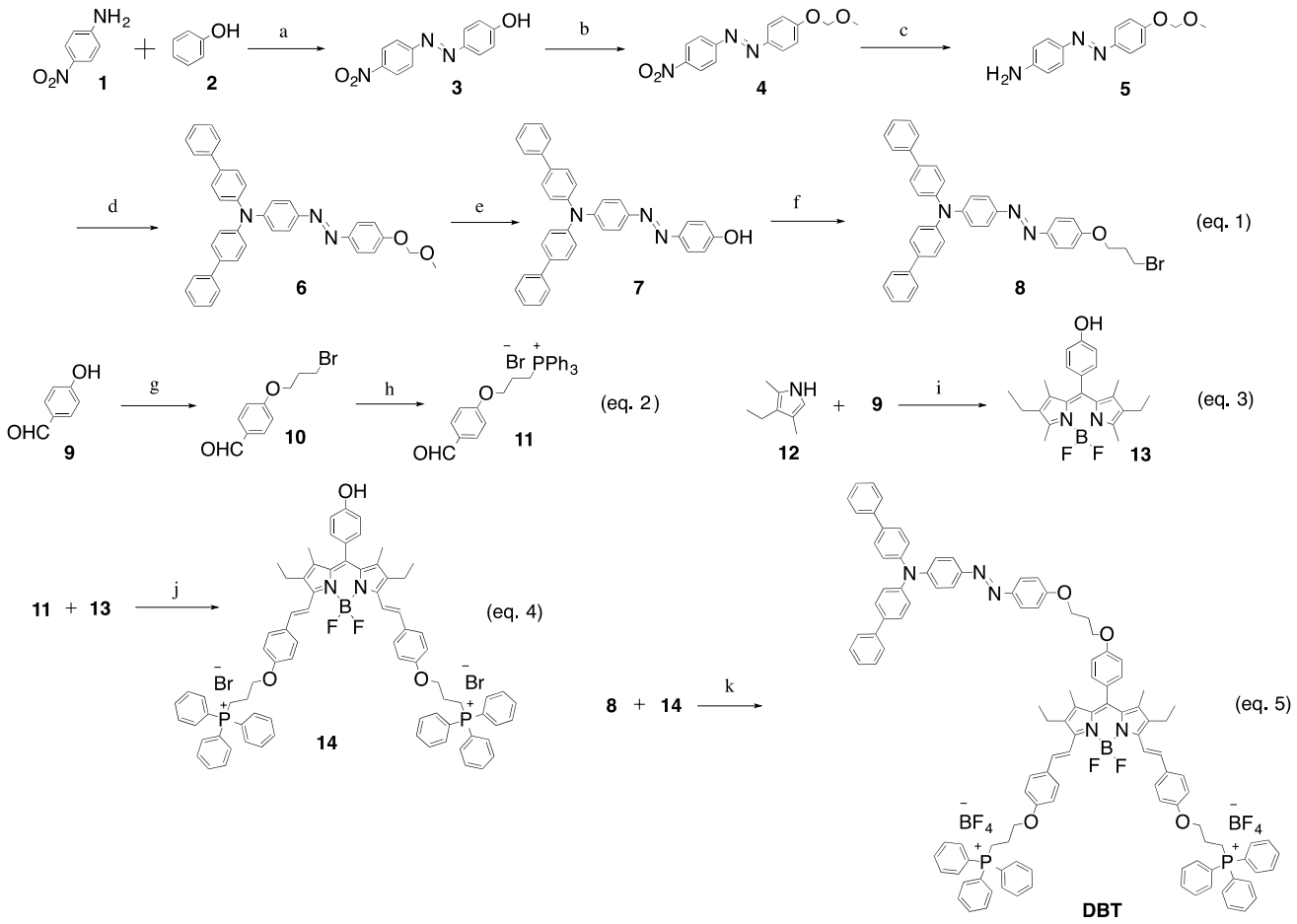

Scheme 1 Synthetic route of **DBT**: (Eq. 1) **a** HCl, $NaNO_2$, H_2O, < 5 °C, 2 h, 96%; **b** $ClCH_2OCH_3$, DIPEA, CH_2Cl_2, 2 h, 87%; **c** $Na_2S{\cdot}9H_2O$, $EtOH/H_2O$, 12 h, 99%; **d** 4-iodobiphenyl, Cu, KOH, decaline, 180 °C, 24 h, 35%; TFA, CH_2Cl_2, r. t., 24 h, 83%; **f** $Br(CH_2)_3Br$, K_2CO_3, acetone, 3 h, 88%; (Eq. 2) **g** $Br(CH_2)_3Br$, K_2CO_3, acetone, 3 h, 83%; **h** PPh_3, toluene, reflux, 48 h, 87%; (Eq. 3) **i** TFA, chloranil, DIPEA, $BF_3{\cdot}OEt_2$, CH_2Cl_2, 84%; (Eq. 4) **j** PTSA, piperidine, toluene, 80 °C, 55%; (Eq. 5) **k** (i) K_2CO_3, acetone, reflux, 13 h; (ii) $NaBF_4$, CH_2Cl_2, r. t., 3 h, 16%

derivative **3** was synthesized by diazo-coupling reaction (Parker et al. 2010). Protection of phenolic hydroxyl group gave **4** followed by reduction of nitro group of **4** to amino group to give **5**. Ullmann amination of **5** with 4-iodobiphenyl using Cu powder and KOH gave **6**. Subsequently, deprotection of **6** was performed to give DBAB unit **7** (Tanino et al. 2007; Nakano et al. 2012). Williamson-ether reaction with excess amount of 1,3-dibromopropane afforded mono ether **8**, selectively (Scheme 1 Eq. 1). Similarly, Williamson-ether synthesis with 4-hydroxybenzaldehyde **9** and excess 1,3-dibromopropane afforded monoether **10**. Subsequently, nucleophilic-substitution reaction **10** and triphenylphosphine gave triphenylphosphonium salt **11** (Scheme 1 Eq. 2). BODIPY derivative **13** synthesized from 3-ethyl-2,4-dimethylpyrrole **12** and **9** (Scheme 1 Eq. 3). Knoevenagel condensation reaction of **11** and **13** afforded **14**, an extension of the π-conjugation, having BODIPY skeleton and two phosphonium moieties (Scheme 1 Eq. 4) (Kolemen et al. 2011). Finally, condensation of **8** and **14** afforded **DBT** framework, followed by treatment with $NaBF_4$ for counter anion exchange was carried out. **DBT** was characterized by ^1H, ^{13}C, ^{19}F and ^{31}P NMR HRMS. The data obtained are in good agreement with the proposed structure. The details are shown in ESI.

Photoisomerization of azobenzene derivatives

For all photoisomerization experiment using by UV–Vis absorption spectra change, photo-irradiation was performed by placing the sample solution 1500 µl (1–30 µM in DMSO) in a quartz cell at 1 cm distance from a slit lens of Xe lamp for 5 min (150W Xe lamp in F-7000; Hitachi fluorescent spectrometer, irradiation of trans to cis at 450 nm, those of cis to trans at 550 nm). Time interval between the UV–Vis absorbance measurements is 30–60 s. Quantum yields were

determined with a Otsuka Electronics QE-2000 calibrated integrating sphere system.

Preparation of GUVs containing DBT

Stock solution of **DBT** 30 µl (500 µM, DMSO) was added to disposable culture tubes. The sample was freeze-dried at -40 °C, < 10 Pa for 1 day. After freeze-dry, EYPC (ca. 0.5–3.0 mg) as a phospholipid and cholesterol (ca. 0.1 mg) is dissolved in dichloromethane (1000 µl) in disposable culture tubes. The solution of lipid and dichloromethane is deposited on a solid substrate, and then only the dichloromethane gradually evaporated by spraying nitrogen gas. After complete evaporation of the dichloromethane, a lipid dry film remains on the substrate. The lipid dry film is gently hydrated by ultrapure water (1 ml). After the sample is allowed to stand for 1 h. at 80 °C, GUVs containing **DBT** are spontaneously formed.

Photoisomerization effects of GUVs containing DBT

The GUVs containing **DBT** solution were then collected by 200 µL in dish with grid, after allowed to stand for 60 min to started observation. For the experiment involving sedimentation in GUVs including **DBT** solution was exposed to 473 nm polarized laser for 1 h using a semiconductor polarized laser (80 mW cm^{-2}) placed 3 cm above the sample. The time interval between the snapshots is 1 min. The sedimentation, photo-irradiation and observation were then performed in the dark.

Cell culture

HepG2 cells were cultured in Dulbecco's modified Eagle's medium (DMEM, Sigma) containing 10% fetal clone III (FC III) and antibiotics in a humidified 5% CO_2 incubator (Thermo) at 37 °C.

Evaluation of localization of DBT in living cell

HepG2 cells were incubated in glass cover slips one day before imaging. For live imaging, 2 mL of Hanks' balanced salt solution (HBSS) containing **DBT** (5 µM), LysoTracker® Green (25 nM) and 2% DMSO was prepared. Subsequently, the cells were incubated with this solution for 15 min at 37 °C. After incubation, the incubation medium was removed and washed twice with 2 mL of HBSS. After standing for 10 min, fluorescence images were captured with a cooled digital CCD camera (ORCA-ER, Hamamatsu Photonics) attached to an inverted fluorescence microscope (Axiovert 135, Carl Zeiss), using band pass filter for **DBT** $\lambda_{ex} = 542–582$ nm and $\lambda_{em} = 604–644$ nm; Lysotracker® Green $\lambda_{ex} = 459–481$ nm and $\lambda_{em} = 499–529$ nm of fluorescence microscope.

Photoisomerization effects of HepG2 cells containing DBT

Two mL of HBSS solution containing **DBT** (5 µM) and 1% DMSO was prepared as an incubation medium. Subsequently, the cells were incubated for 15 min at 37 °C. After incubation, the incubation medium was removed from the dish and the cells were washed twice with 2 mL HBSS. After standing for 10 min, fluorescence images of the cells were captured, using band pass filter for **DBT** $\lambda_{ex} = 542–582$ nm and $\lambda_{em} = 604–644$ nm.

For the experiment involving sedimentation in HepG2 cells including **DBT** was exposed to 473 nm polarized laser for 20 min using a semiconductor polarized laser (80 mW cm^{-2}) placed 3 cm above the sample. The time interval between the snapshots is 4 min. The sedimentation, photo-irradiation and observation were then performed in the dark.

Trypan blue staining

After irradiation to HepG2 cells containing **DBT**, the cells were stained with 0.2% Trypan Blue solution (50% HBSS buffer). After incubation for 1 min, the cell culture was washed twice with HBSS (2 mL).

Photoreaction of diphenylbenzofuran DPBF in the presence of DBT

A solution of **DPBF** in DMSO (30 µM, 2.0 ml) in the presence or absence of **DBT** (10 µM) was irradiated with 473 or 562 nm light in a quartz cell at room temperature for 10 min under air bubbling. After irradiating, the fluorescence intensity of **DPBF** was measured by fluorescence spectrophotometer.

Results and discussion

The UV–Vis and fluorescence spectrum of **DBT** was compared to azobenzene AB, DBAB, **13** and **14**. A π–π^* transition absorption of DBAB moiety in **DBT** was observed at 434 nm in DMSO solution. Comparing to that of AB (317 nm), the absorption was redshifted by the influence of the dibiphenylamino group and reached the visible-light region. In **13** and **14** having BODIPY skeleton, absorption maximum wavelength was observed at 525, 654 nm, and fluorescence wavelength was observed at 543, 683 nm, respectively. By combining two styryl groups as conjugating side chains in the BODIPY moiety, the conjugation of **14** is

Table 1 Photophysical properties of **DBT** and related compounds[a]

Compd	λ_{abs} (nm)[c]	ε ($\chi\mu^{-1}$ M^{-1})[d]	λ_{em} (nm)[e]	K ($\chi\mu^{-1}$)[f]	Φ_f[g]
DBAB	441	14,392	–	–	–
13	525	39,058	543	628	0.80
14	654	68,574	683	649	0.52
DBT	656	55,697	686	667	0.60

All data were measured in DMSO

[b]Synthesized according to the literature

[c]Absorption maxima peak in nm unit

[d]Molar absorptivity

[e]Fluorescence maxima peak in nm unit

[f]Stokes shift in nm unit

[g]Quantum yield

expanded, and a significant redshift occurs in both absorption and fluorescence as compared with **13**. Similarly, the absorption maximum wavelength was observed at 656 nm, and the maximum fluorescence of **DBT** was observed at 686 nm with a Stoke shift of 667 cm^{-1} (Table 1). DBAB and BODIPY exist independently in optical characteristics in **DBT**.

DBT was dissolved in DMSO and photoisomerization measurements were performed by photo-irradiation using a xenon lamp at 450 nm and 550 nm. The absorption spectra after irradiation per unit time were measured. In the UV–Vis spectrum of **DBT**, strong π–π* transition absorption from trans-DBAB and weak n–π* transition absorption at around 550 nm were observed at around 450 nm (Fig. 2). By irradiating 450 nm light, a decrease in absorption band around 450 nm and a slight increase in absorption band around 550 nm were observed to confirm photoisomerization to *cis*-DBAB (Fig. 2. left). By irradiating 550 nm light, the isomerization to *trans*-DBAB was observed (Fig. 2. right). These results suggest that reversible photoisomerization of **DBT** occurs similarly to other azobenzene derivatives (Ando et al. 2003; Tanino et al. 2007; Nakano et al. 2012).

GUVs containing **DBT** were prepared by natural swelling method (Hishida 2010), and localized portions of **DBT** were observed using a fluorescence microscopic analysis. GUVs for fluorescence observation were prepared using DOPC as lipids. The result suggests that **DBT** was localized between hydrophobic membranes of vesicles due to the influence of the hydrophobic moiety possessed by **DBT** (Fig. 3).

DBT was introduced into GUVs prepared from EYPC, and laser light (473 nm, 80 mW) was irradiated to the GUVs, and morphological change of vesicles was observed with an optical microscope at a minute interval. GUVs containing **DBT** and cholesterol were prepared by natural swelling method in the similar way as fluorescence observation and **DBT** (500 nM) was also added to the solution to observe morphological change (Fig. 4a). As a result, before the start

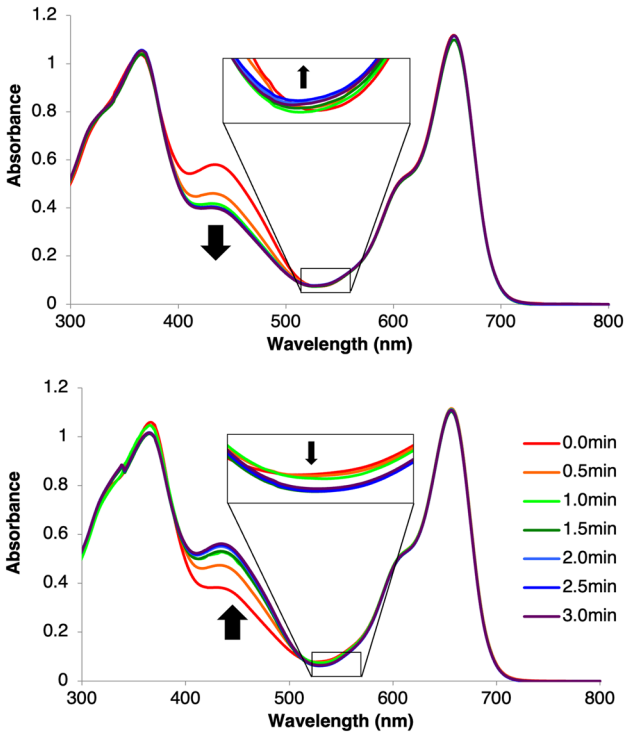

Fig. 2 UV–Vis spectra of **DBT** in DMSO after irradiation at 450 nm for 0.0, 0.5, 1.0, 1.5, 2.0, 2.5, 3.0 min (top) and after irradiation at 550 nm for 0.0, 0.5, 1.0, 1.5, 2.0, 2.5, 3.0 min (bottom). The inset shows the n–π* transition appears as a weak band at around 530 nm

of the observation, it was a perfect round sphere without distortion, but it was able to observe the morphological change that causes distortion gradually as light irradiation. Ultimately, the division of the vesicle was seen (Fig. 4b). Such morphological changes due to light irradiation could be confirmed by several vesicles in the other fields (Ishii et al. 2009; Diguet et al. 2012; Pernpeintner et al. 2017; Liu et al. 2017).

Furthermore, the morphological changes of vesicles by irradiation were monitored using fluorescence microscopy (Fig. 5). At first, the vesicle, which was a sphere (Fig. 5a), was immediately deformed by 473 nm light irradiation (Fig. 5b). In addition, when the vesicle was irradiated with 562 nm light, which is the isomerization wavelength from the *cis* to the *trans*-form, the strain was eliminated and returned to the sphere such as before irradiation (Fig. 5c). This phenomenon seems to cause morphological changes with the structural change of **DBT**, which was all *trans*-form before light irradiation, by the isomerization to the *cis*-form. In addition, 562 nm light irradiation was caused by photoisomerization to the *trans*-form, and the distortion was eliminated by returning to the same state as before irradiation. It is considered that reversible morphological change was observed by causing destabilization of the membrane structure along with photoisomerization of **DBT** localized

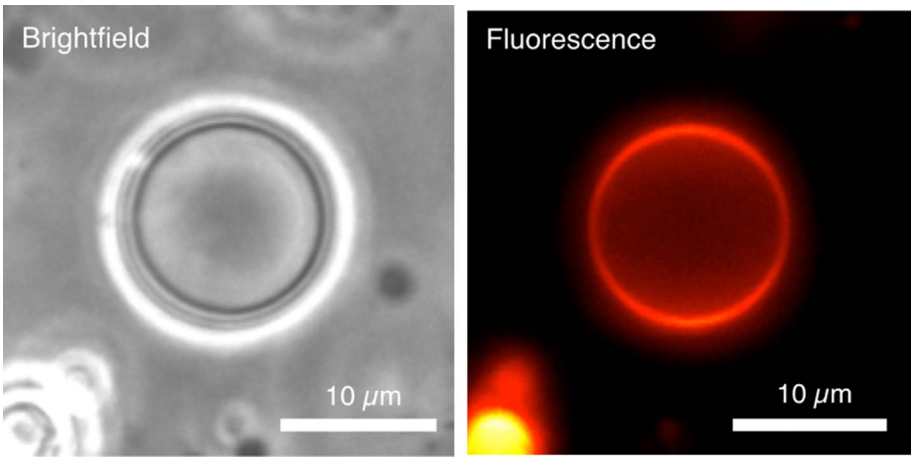

Fig. 3 Microscope images of GUVs containing **DBT**: Bright-field image (left); fluorescent image of **DBT** (right); GUVs are made from DOPC with **DBT**

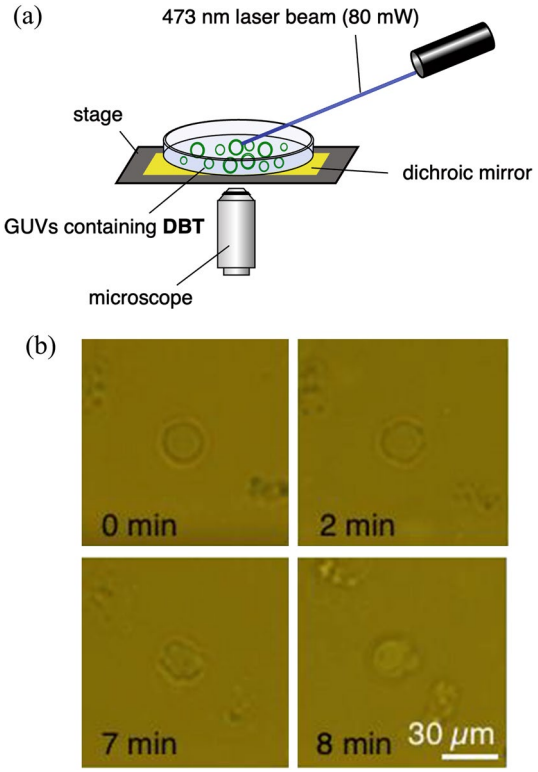

Fig. 4 **a** Experimental setup for observation effect of GUVs containing **DBT** by irradiation of laser beam at 473 nm. **b** Microscopic images with irradiation polarized laser at 473 nm to GUVs containing **DBT** for $t = 0$, 2, 7 and 8 min. GUVs are made from EYPC with **DBT** and cholesterol

to the hydrophobic part of the vesicle with the TPP moiety oriented outer sphere.

DBT was loaded into living cells and localized sites were identified using a fluorescence microscope. HepG2 cells which are cancer cells derived from human liver cancer were used as biological samples. When **DBT** was introduced into this cell, uptake into the cell was confirmed. Double-staining experiments of **DBT** with MitoTracker® Green for mitochondria or LysoTracker® Green for lysosome were carried out. As shown in Figure S1, the fluorescence signals of **DBT** were not merged with mitochondria even though **DBT** is conjugated with TPP. The **DBT** signals were co-localized with lysosomes incubated at 37 °C (Fig. 6), whereas the uptake of **DBT** was dramatically inhibited at 4 °C (Figure S2). Basically, endocytosis is known as a temperature-dependent process and is inhibited at low temperatures. Thus, these results show that **DBT** was probably internalized into cells via an endocytic pathway and then localized to lysosomes without endosomal escape.

Furthermore, changes in cell morphology due to light irradiation were examined with a fluorescence microscope equipped with a laser light irradiation (473 nm, 30 mW) device. HepG2 cells containing **DBT** were irradiated for cumulative irradiation time of 20 min and the morphological change of the cells was followed with a fluorescence microscope. As the irradiation time became longer, the morphology of the lysosome derived from the fluorescence emission of **DBT** gradually became blurred, and the morphological change due to the damage of the whole cell was observed (Fig. 7a). After light irradiation, Trypan Blue staining, which is a dead cell stain, was carried out, and it showed a positive reaction only in the region irradiated with light (Fig. 7b). As control experiments, no influence of cells was observed even when HepG2 cells without up-taking **DBT** were irradiated with 473 nm laser light (Figure S4). Furthermore, a compound having two TPP and BODIPY skeletons and not having DBAB (**15**) was also synthesized. Cell death

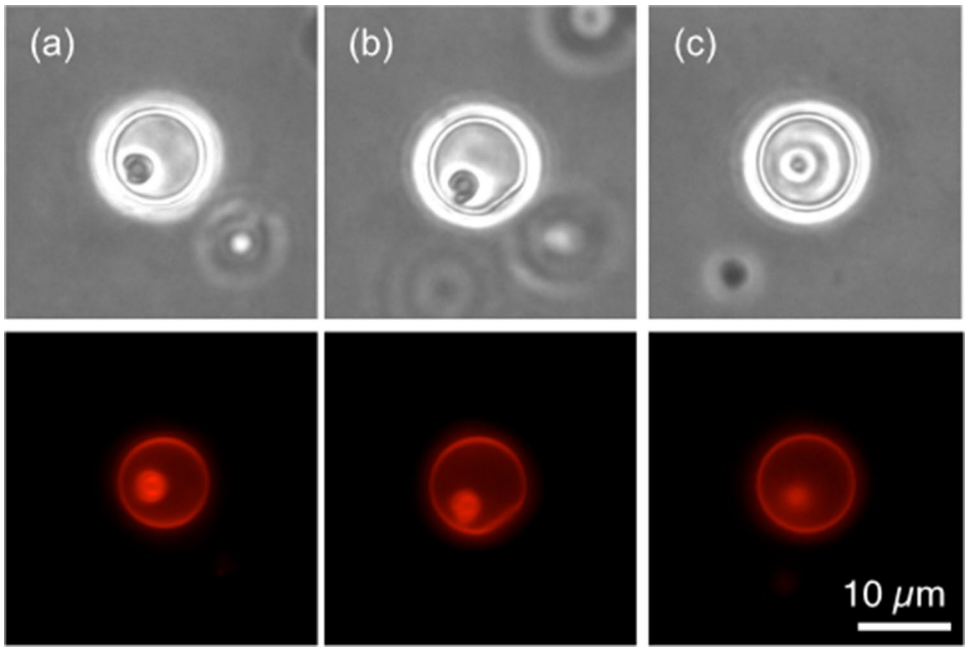

Fig. 5 Microscopic images (top) and fluorescent images (bottom) of GUVs containing **DBT**. The GUVs made from DOPC with **DBT** and cholesterol. **a** Before irradiation; **b** Irradiation at 473 nm for 1 min; **c** Irradiation at 562 nm for 1 min

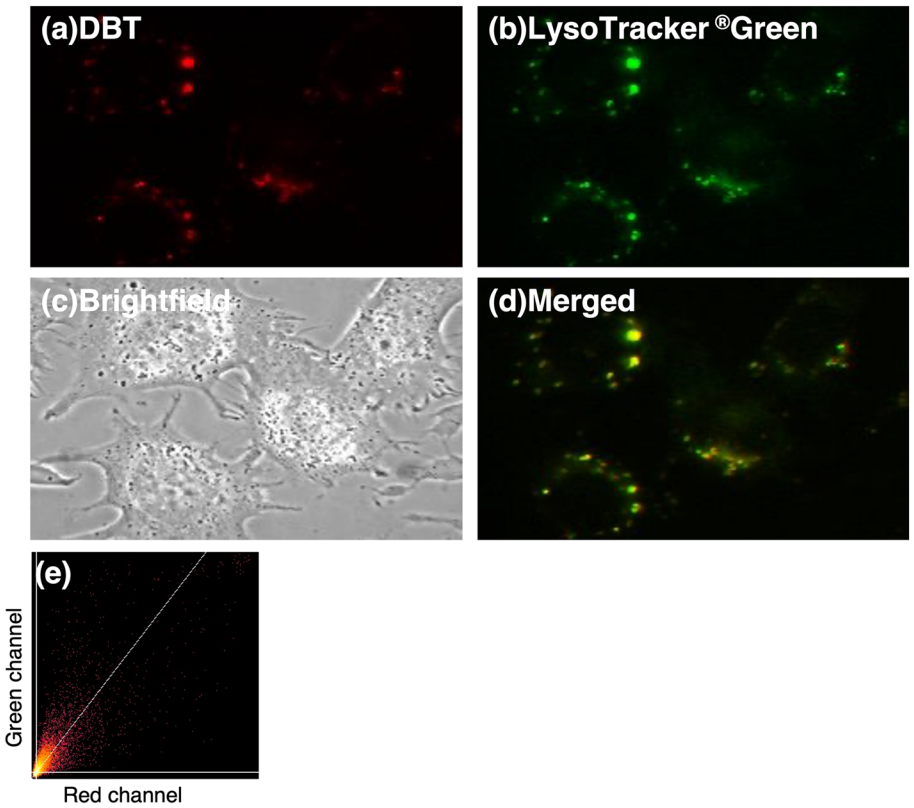

Fig. 6 Fluorescence images of HepG2 cells loaded **DBT** and LysoTracker® Green were loaded. **a** Fluorescence image of **DBT** (5 μM); **b** Fluorescent image of LysoTracker® Green (25 nM); **c** Brightfield image; **d** Merged image. Scale bar is 20 μm. **e** Pearson correlation ($r = 0.829$)

was not induced by light irradiation of HepG2 cells into which the compound was loaded (Figure S5). Cytotoxicity of **DBT** was also checked by CCK-8 assay. As a result, **DBT** was not cytotoxic at least up to 10 μM. That is, the observed cell death was found to be induced by DBAB moiety in the **DBT** molecule and light irradiation on it.

As a factor causing cell death by photo-irradiating cells to which fluorescent dye has been loaded, it is considered that the loaded dye acts as a photosensitizer to generate singlet oxygen, and the chemical species causes cell death. Using singlet oxygen detection reagent DPBF, **DBT** solution was irradiated with light to investigate whether or not singlet

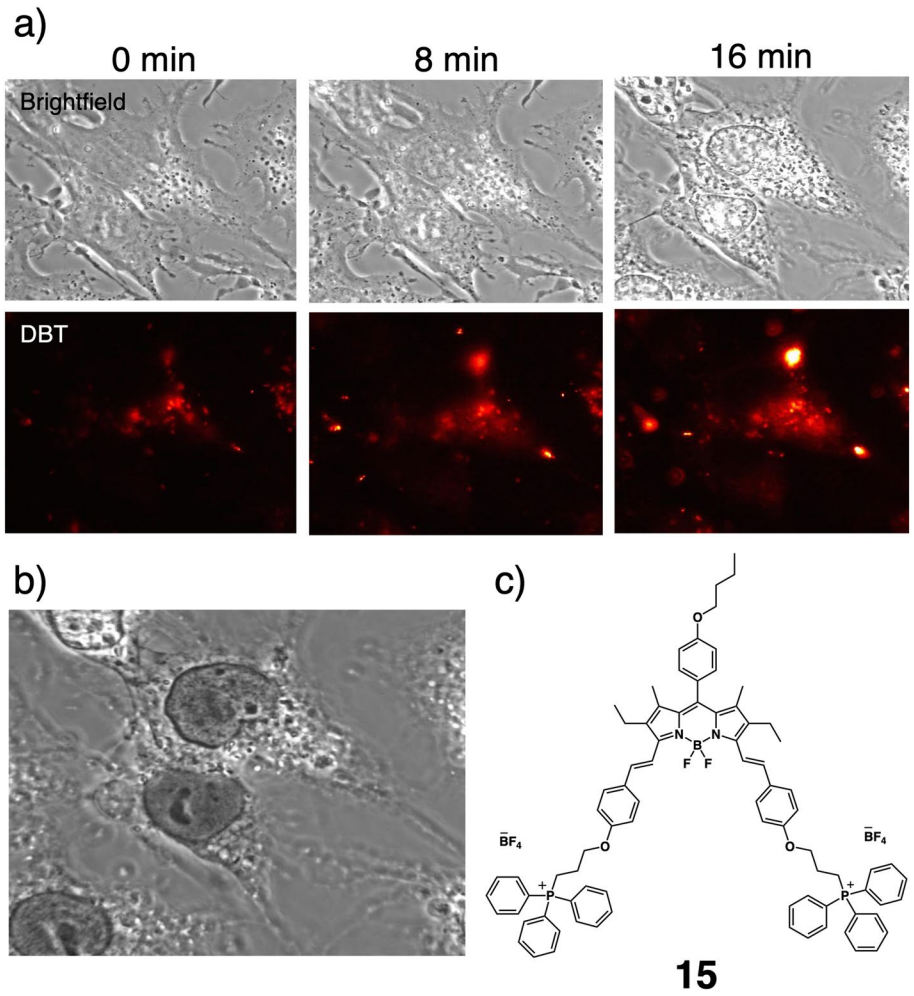

Fig. 7 **a** Microscopic image of the change in cell morphology after irradiation polarized laser at 473 nm to HepG2 cells containing **DBT** for t = 0, 12 and 20 min. **b** Trypan Blue staining after 20 min of light irradiation. **c** Structure of compound **15**

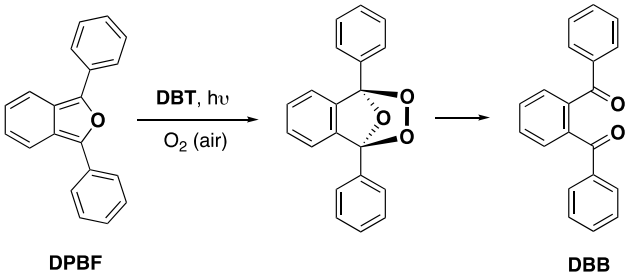

Scheme 2 Photoreaction of DPBF with $^1O_2$ in the presence of **DBT**

oxygen was generated. DPBF reacts with singlet oxygen to produce 1,2-dibenzoylbenzene DBB (Zhang and Yang 2013; Zhang et al. 2013), which reduces the intensity of fluorescence originated from DPBF (Scheme 2).

When only DPBF was irradiated with 473 nm light under an oxygen atmosphere, the decreasing rate of the fluorescence intensity derived from DPBF was 6.75%, and the decreasing rate of the fluorescence intensity was 8.23% even when irradiated with 562 nm light. This decrease in fluorescence intensity is considered to be due to self-bleaching of DPBF.

Table 2 Generation of singlet oxygen with photo-irradiation for **DBT** in DMSO

	Irradiation light λ [nm]	Decreasing rate ΔF_{460} [%]
DPBF	473	6.57
DPBF + **DBT**		4.44
DPBF	562	8.23
DPBF + **DBT**		19.17

On the other hand, when **DBT** was added to a DMSO solution containing DPBF and irradiated with light having a wavelength of 562 nm, a clear decrease in the fluorescence derived from DPBF could be confirmed. However, even when irradiated with light with a wavelength of 473 nm, no significant decrease in fluorescence intensity could be observed (Table 2).

This result indicates that **DBT** does not generate singlet oxygen even when irradiated with DBAB π–π^* transition

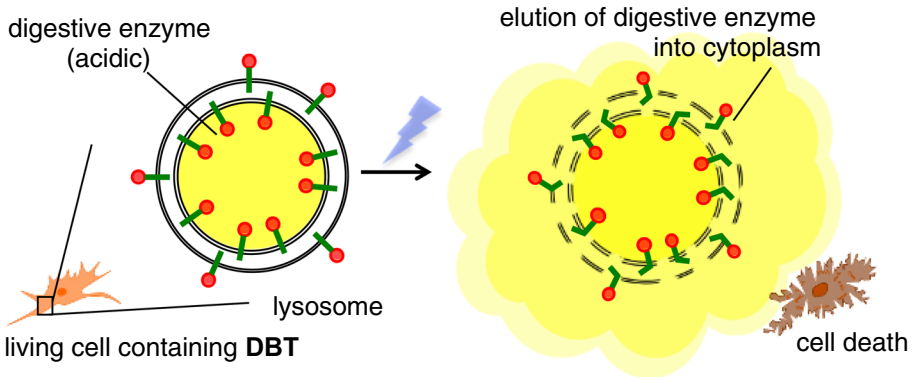

Fig. 8 The proposed mechanism of cell death by photoisomerization of **DBT** in lysosome

absorption wavelength light. BODIPY absorbs light of its excitation wavelength and generates singlet oxygen by energy transfer accompanying collision with dissolved oxygen. It is known that the generated singlet oxygen reacts with the BODIPY dye itself, which causes bleaching with decomposition of the dye (Scholz et al. 2013; Mula et al. 2008). This breaching of **DBT** was not observed when light of 473 nm laser irradiates to **DBT** solution or living cell containing **DBT**.

When trans–cis isomerization light is irradiated to GUV into which the azo compound of the *trans*-form is inserted, a *cis*-form having a lower hydrophobicity than the *trans*-form is generated and released to the outside of the membrane, and disturbs the lipid organization, which results in GUV bursting (Suzuki et al. 2017). Based on our findings, the influence of **DBT** on living cells is considered as follows. In lysosomes localizing **DBT**, acidic encapsulated liquid containing various digestive enzymes has been separated from cytoplasm by biological membrane. **DBT** with a hydrophobic moiety is localized in the lipid membrane of the lysosome, and photoisomerization of the DBAB moiety of **DBT** causes destabilization of the membrane structure. As a result, lysosomal contents are eluted into the cytoplasm, cell homeostasis is not able to be maintained and cell death is caused (Fig. 8).

Conclusions

An azobenzene derivative having cell membrane permeability and optically independent fluorophore was synthesized. This compound underwent photoisomerization, which in turn affected the stability of lipid membranes. This destabilization causes collapse of cellular homeostasis. Photodynamic therapy known as one of cancer therapeutic methods generates singlet oxygen and/or free radicals in cells using a sensitizer to damage cancer cells. It is revealed that the synthesized compound damaged the cells without generating reactive highly active chemical species by light irradiation.

Supplementary Information The online version contains supplementary material available at https://doi.org/10.1007/s11696-023-02685-8.

Declarations

Conflict of interest On behalf of all authors, the corresponding author states that there is no conflict of interest.

References

Ando H, Takahashi T, Nakano H, Shirota Y (2003) Comparative studies of the formation of surface relief grating. Amorphous molecular material vs vinyl polymer. Chem Lett 32:710–711

Banghart M, Borges K, Isacoff E, Trauner D, Kramer RH (2004) Light-activated ion channels for remote control of neuronal firing. Nat Neurosci 7:1381–1386

Bandara HMD, Burdette SC (2012) Photoisomerization in different classes of azobenzene. Chem Soc Rev 41:1809–1825

Beharry AA, Sadovski O, Woolley GA (2011) Azobenzene photoswitching without ultraviolet light. J Am Chem Soc 133(49):19684–19687

Boens N, Leen V, Dehaen W (2012) Fluorescent indicators based on BODIPY. Chem Soc Rev 41:1130–1172

Brenner S (1974) The genetics of *Caenorhabditis elegans*. Genetics 77:71–94

Diguet A, Yanagisawa M, Liu YJ, Brun E, Abadie S, Rudiuk S, Baig D (2012) UV-induced bursting of cell-sized multicomponent lipid vesicles in a photosensitive surfactant solution. J Am Chem Soc 134:4898–4904

Felício MR, Silva ON, Gonçalves S, Santos NC, Franco OL (2017) Peptides with dual antimicrobial and anticancer activities. Front Chem 21:1–9

Green K, Brand MD, Murphy MP (2004) Prevention of mitochondrial oxidative damage as a therapeutic strategy in diabetes. Diabetes 53(suppl 1):S110–S118

Hartley GS (1937) The cis-form of azobenzene. Nature 281281

Hishida M (2010) Formation mechanism of giant phospholipid vesicles under natural swelling. Philos Nat SP1–13

Hartwell LH (1991) Twenty-five years of cell cycle genetics. Genetics 4:975–980

Hamada T, Sato YT, Yoshikawa K, Nagasaki T (2005) Reversible photoswitching in a cell-sized vesicle. Langmuir 21(17):7626–7628

Ishii K, Hamada T, Hatakeyama M, Sugimoto R, Nagasaki T, Takagi M (2009) Reversible control of exo- and endo-budding transitions in a photosensitive lipid membrane. ChemBioChem 10:251–256

Kasai K, Nagahora N, Okuma K, Matsubara K, Shioji K (2022) Photo-induced morphological changes of lipid bilayer vesicles enabled by a visible-light-responsive azo compound. J Oleo Sci 71(5):747–757

Kolemen S, Bozdemir OA, Cakmak Y, Barin G, Ela SE, Marszalek M, Yum JH, Zakeeruddin SM, Nazeeruddin MK, Grätzel M, Akkaya EU (2011) Optimization of distyryl-Bodipy chromophores for efficient panchromatic sensitization in dye sensitized solar cells. Chem Sci 2:949–954

Kuruvilla FG, Shamji AF, Sternson SM, Hergenrother PJ, Schreiber SL (2002) Dissecting glucose signalling with diversity-oriented synthesis and small-molecule microarrays. Nature 416:653–657

Lee KM, White TJ (2012) Photochemical mechanism and photothermal considerations in the mechanical response of monodomain, azobenzene-functionalized liquid crystal polymer networks. Macromolecules 45(17):7163–7170

Lin YL, Chang HY, Sheng YJ, Tsao HK (2012) Photoresponsive polymersomes formed by amphiphilic linear-dendritic block copolymers: generation-dependent aggregation behavior. Macromolecules 45(17):7143–7156

Liu D, Wang S, Xu S, Liu H (2017) Photocontrollable intermittent release of doxorubicin hydrochloride from liposomes embedded by azobenzene-contained glycolipid. Langmuir 33(4):1004–1012

Loudet A, Burgess K (2007) BODIPY dyes and their derivatives: syntheses and spectroscopic properties. Chem Rev 107:4891–4932

Merino E, Ribagorda M (2012) Control over molecular motion using the *cis-trans* photoisomerization of the azo group. Belistein J Org Chem 8:1071–1090

Mula S, Ray AK, Banerjee M, Chaudhuri T, Dasgupta K, Chattopadhyay S (2008) Design and development of a new pyrromethene dye with improved photostability and lasing efficiency: theoretical rationalization of photophysical and photochemical properties. J Org Chem 73:2146–2154

Muraoka T, Kinbara K, Kobayashi Y, Aida T (2003) Light-driven open-close motion of chiral molecular scissors. J Am Chem Soc 125:5612–5613

Nakano H, Suzuki M (2012) Photoinduced mass flow of photochromic molecular materials. J Mater Chem 22:3702–3704

Parker RM, Gates JC, Rogers HL, Smith PGR, Grossel MC (2010) Using the photoinduced reversible refractive-index change of an azobenzene co-polymer to reconfigure an optical Bragg grating. J Mater Chem 20:9118–9125

Pernpeintner C, Frank JA, Urban P, Roeske CR, Pritzl SD, Trauner D, Lohmüller T (2017) Light-controlled membrane mechanics and shape transitions of photoswitchable lipid vesicles. Langmuir 33(16):4083–4089

Samanta S, Beharry AA, Sadovski O, McCormick TM, Babalhavaeji A, Tropepe V, Woolley GA (2013) Photoswitching azo compounds in vivo with red light. J Am Chem Soc 135(26):9777–9784

Samundeeswari S, Chougala B, Holiyachi M, Shastri L, Kulkarni M, Dodamani S, Jalalpur S, Joshi S, Dixit S, Sunagar V, Hunnur R (2017) Design and synthesis of novel phenyl-1,4-beta-carboline-hybrid molecules as potential anticancer agents. E J Med Chem 128:123–139

Schreiber SL (2003) The small-molecule approach to biology: chemical genetics and diversity-oriented organic synthesis make possible the systematic exploration of biology. Chem Eng News 81:51–61

Scholz M, Dědic R, Breitenbach T, Hála J (2013) Singlet oxygen-sensitized delayed fluorescence of common water-soluble photosensitizers. Photochem Photobiol Sci 12:1873–1884

Sebai SC, Cribier S, Karimi A, Massotte D, Tribet C (2010) Permeabilization of lipid membranes and cells by a light-responsive copolymer. Langmuir 26(17):14135–14141

Shinkai S, Minami T, Kusano Y, Manabe O (1983) Photoresponsive crown ethers. 8. Azobenzenophane-type "switched-on" crown ethers which exhibit an all-or-nothing change in ion-binding ability. J Am Chem Soc 105:1851–1856

Stockwell BR (2000) Chemicalgenetics:ligand-based discovery of gene function. Nature Rev Genet 1:116–125

Stockwell BR (2004) Exploring biology with small organic molecules. Nature 432:846–854

Sun K, Chen K, Xue G, Cai J, Zou G, Li Y, Zhang Q (2013) Near-infrared light induced fusion and fission of azobenzene-containing polymer vesicles. RSC Adv 3:23997–24000

Suzuki Y, Okuro K, Takeuchi T, Aida T (2012) Friction-mediated dynamic disordering of phospholipid membrane by mechanical motions of photoresponsive molecular glue: activation of ion permeation. J Am Chem Soc 134:15273–15276

Suzuki Y, Nagai KH, Zinchenko A, Hamada T (2017) Photoinduced fusion of lipid bilayer membranes. Langmuir 33(10):2671–2676

Tacar O, Sriamornsak P, Dass CR (2012) Doxorubicin: an update on anticancer molecular action, toxicity and novel drug delivery systems. J Pharm Pharmacol 65:157–170

Tanino T, Yoshikawa S, Ujike T, Nagahama D, Moriwaki K, Takahashi T, Kotani Y, Nakano H, Shirota Y (2007) Creation of azobenzene-based photochromic amorphous molecular materials-synthesis, glass-forming properties, and photochromic response. J Mater Chem 17:4953–4963

Tokala R, Thatikonda S, Sana S, Regur P, Godugu C, Shankaraiah N (2018) Synthesis and in vitro cytotoxicity evaluation of β-carboline-linked 2,4-thiazolidinedione hybrids: potential DNA intercalation and apoptosis-inducing studies. New J Chem 42:16226–16236

Ulrich G, Ziessel R, Harriman A (2008) The chemistry of fluorescent bodipy dyes: versatility unsurpassed. Angew Chem Int Ed 47:1184–1201

Wang X, Yin J, Wang X (2011) Self-structured surface patterns on epoxy-based azo polymer films induced by laser light irradiation. Macromolecules 44(17):6856–6867

Yu Y, Nakano M, Ikeda T (2003) Directed bending of a polymer film by light. Nature 425:145

Zhang XF, Yang X (2013) Singlet oxygen generation and triplet excited-state spectra of brominated BODIPY. J Phys Chem B 117:5533–5539

Zhang S, Wu T, Fan J, Li Z, Jiang N, Wang J, Dou B, Sun S, Song F, Peng X (2013) A BODIPY-based fluorescent dye for mitochondria in living cells, with low cytotoxicity and high photostability. Org Biomol Chem 11(4):555–558

Zhang L, Liu W, Huang X, Zhang G, Wang X, Wang Z, Zhang D, Jiang X (2015) Old is new again: a chemical probe for targeting mitochondria and monitoring mitochondrial membrane potential in cells. Analyst 140:5849–5854